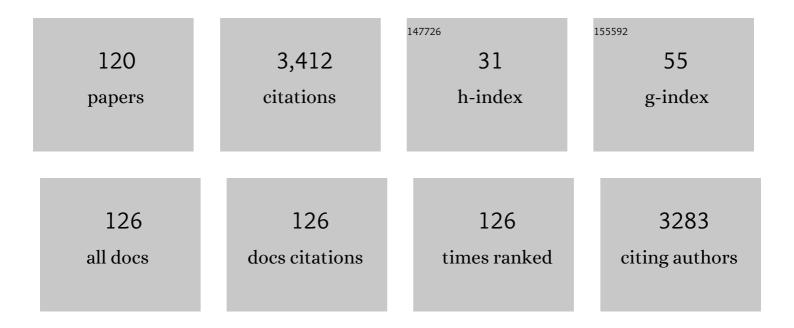
## Esteban Broitman

List of Publications by Year in descending order

Source: https://exaly.com/author-pdf/8749552/publications.pdf Version: 2024-02-01



ESTERAN BROITMAN

#	Article	lF	CITATIONS
1	The influence of steel microstructure in high-speed high-load bearing applications. Materials Science and Technology, 2021, 37, 1370-1385.	0.8	4
2	Reactive sputtering of CSx thin solid films using CS2 as precursor. Vacuum, 2020, 182, 109775.	1.6	13
3	Measurement of H and E within and in the neighborhood of a single hydride platelet in Zircaloy-2. Journal of Nuclear Materials, 2020, 531, 152013.	1.3	3
4	Adaptive hard and tough mechanical response in single-crystal B1 VNx ceramics via control of anion vacancies. Acta Materialia, 2020, 192, 78-88.	3.8	46
5	Micro and Macro-Tribology Behavior of a Hierarchical Architecture of a Multilayer TaN/Ta Hard Coating. Coatings, 2020, 10, 263.	1.2	10
6	Tribological and nanomechanical properties of a lignin-based biopolymer. E-Polymers, 2020, 20, 528-541.	1.3	2
7	Reactive magnetron sputtering of tungsten target in krypton/trimethylboron atmosphere. Thin Solid Films, 2019, 688, 137384.	0.8	6
8	Nanomechanical and microtribological properties of yttrium thin films for photocathode engineering. Journal of Vacuum Science and Technology A: Vacuum, Surfaces and Films, 2019, 37, 031507.	0.9	0
9	Tribological and Nanomechanical Behavior of Liquid Wood. Journal of Tribology, 2019, 141, .	1.0	8
10	Synthesis and characterization of (Ti1-Al )B2+ thin films from combinatorial magnetron sputtering. Thin Solid Films, 2019, 669, 181-187.	0.8	24
11	Advances in science and technology of polymers and composite materials. E-Polymers, 2018, 18, 1.	1.3	3
12	Growth and mechanical properties of 111-oriented V0.5Mo0.5Nx/Al2O3(0001) thin films. Journal of Vacuum Science and Technology A: Vacuum, Surfaces and Films, 2018, 36, .	0.9	15
13	Micro-tribological performance of fullerene-like carbon and carbon-nitride surfaces. Tribology International, 2018, 128, 104-112.	3.0	11
14	Mechanical and Tribological Properties of the Oxide Thin Films Obtained by Sol-Gel Method. , 2018, , 1513-1526.		0
15	V0.5Mo0.5Nx/MgO(001): Composition, nanostructure, and mechanical properties as a function of film growth temperature. Acta Materialia, 2017, 126, 194-201.	3.8	23
16	Synthesis and characterization of the mechanical and optical properties of Ca-Si-O-N thin films deposited by RF magnetron sputtering. Surface and Coatings Technology, 2017, 315, 88-94.	2.2	11
17	Mechanical and tribological behavior of sol–gel TiO2–CdO films measured at the microscale levels. Journal of Sol-Gel Science and Technology, 2017, 82, 682-691.	1.1	3
18	High temperature nanoindentation hardness and Young's modulus measurement in a neutron-irradiated fuel cladding material. Journal of Nuclear Materials, 2017, 487, 113-120.	1.3	30

ESTEBAN BROITMAN

#	Article	IF	CITATIONS
19	Synthesis and properties of CS <sub><i>x</i></sub> F <sub><i>y</i></sub> thin films deposited by reactive magnetron sputtering in an Ar/SF <sub>6</sub> discharge. Journal of Physics Condensed Matter, 2017, 29, 195701.	0.7	9
20	Growth of lead thin films on silicon and niobium substrates by sputtering technique. Journal of Vacuum Science and Technology A: Vacuum, Surfaces and Films, 2017, 35, 031502.	0.9	4
21	Comparative study of macro- and microtribological properties of carbon nitride thin films deposited by HiPIMS. Wear, 2017, 370-371, 1-8.	1.5	11
22	Diamond graphitization by laser-writing for all-carbon detector applications. Diamond and Related Materials, 2017, 75, 25-33.	1.8	26
23	Indentation Hardness Measurements at Macro-, Micro-, and Nanoscale: A Critical Overview. Tribology Letters, 2017, 65, 1.	1.2	329
24	Innovations in polymers and composite materials. E-Polymers, 2017, 17, 1.	1.3	4
25	Pulsed laser deposition of yttrium photocathode suitable for use in radio-frequency guns. Applied Physics A: Materials Science and Processing, 2017, 123, 1.	1.1	7
26	Age hardening in (Ti 1â^'x Al x )B 2+Δ thin films. Scripta Materialia, 2017, 127, 122-126.	2.6	38
27	Nanotribological behavior of deep cryogenically treated martensitic stainless steel. Beilstein Journal of Nanotechnology, 2017, 8, 1760-1768.	1.5	6
28	Advanced Carbon-Based Coatings. , 2016, , .		0
29	Microstructural, nanomechanical, and microtribological properties of Pb thin films prepared by pulsed laser deposition and thermal evaporation techniques. Journal of Vacuum Science and Technology A: Vacuum, Surfaces and Films, 2016, 34, 021505.	0.9	10
30	ICMCTF 2016 $\hat{a} \in$ " Preface. Surface and Coatings Technology, 2016, 308, 1.	2.2	0
31	Fabrication of Nb/Pb structures through ultrashort pulsed laser deposition. Journal of Vacuum Science and Technology A: Vacuum, Surfaces and Films, 2016, 34, .	0.9	2
32	Hard and elastic epitaxial ZrB2 thin films on Al2O3(0001) substrates deposited by magnetron sputtering from a ZrB2 compound target. Acta Materialia, 2016, 111, 166-172.	3.8	47
33	Mechanical and tribological properties of AlCuFe quasicrystal and Al(Si)CuFe approximant thin films. Journal of Materials Research, 2016, 31, 232-240.	1.2	6
34	Mechanical properties and tribological behavior at micro and macro-scale of WC/WCN/W hierarchical multilayer coatings. Tribology International, 2016, 101, 194-203.	3.0	24
35	Tight comparison of Mg and Y thin film photocathodes obtained by the pulsed laser deposition technique. Nuclear Instruments and Methods in Physics Research, Section A: Accelerators, Spectrometers, Detectors and Associated Equipment, 2016, 836, 57-60.	0.7	7
36	High-temperature nanoindentation of epitaxial ZrB2 thin films. Scripta Materialia, 2016, 124, 117-120.	2.6	25

ESTEBAN BROITMAN

#	Article	IF	CITATIONS
37	Novel transparent MgSiON thin films with high hardness and refractive index. Vacuum, 2016, 131, 1-4.	1.6	16
38	Structural and morphological properties of metallic thin films grown by pulsed laser deposition for photocathode application. Applied Physics A: Materials Science and Processing, 2016, 122, 1.	1.1	5
39	Nanofrictional behavior of amorphous, polycrystalline and textured Y-Cr-O films. Applied Surface Science, 2016, 378, 157-162.	3.1	5
40	Mechanical and Tribological Properties of the Oxide Thin Films Obtained by Sol–gel Method. , 2016, , 1-14.		4
41	Novel insights in polymer and composite materials. E-Polymers, 2015, 15, 285-286.	1.3	2
42	ICMCTF 2015 — Preface. Thin Solid Films, 2015, 596, 1.	0.8	0
43	Analysis of direct and converse piezoelectric responses from zinc oxide nanowires grown on a conductive fabric. Physica Status Solidi (A) Applications and Materials Science, 2015, 212, 579-584.	0.8	14
44	Nanoprobe mechanical and piezoelectric characterization of Sc <i><sub>x</sub></i> Al <sub>1â^'<i>x</i></sub> N(0001) thin films. Physica Status Solidi (A) Applications and Materials Science, 2015, 212, 666-673.	0.8	15
45	2015 Global Conference on Polymer and Composite Materials (PCM2015). IOP Conference Series: Materials Science and Engineering, 2015, 87, 011001.	0.3	0
46	ICMCTF 2015 — Preface. Surface and Coatings Technology, 2015, 284, 1.	2.2	0
47	Characterisation of Pb thin films prepared by the nanosecond pulsed laser deposition technique for photocathode application. Thin Solid Films, 2015, 579, 50-56.	0.8	13
48	Mechanical and tribological properties of CdOÂ+ÂSnO2 thin films prepared by sol–gel. Journal of Sol-Gel Science and Technology, 2015, 74, 114-120.	1.1	18
49	Stresses and Cracking During Chromia-Spinel-NiO Cluster Formation in TBC Systems. Journal of Thermal Spray Technology, 2015, 24, 1002-1014.	1.6	18
50	Nanomechanical and electrical properties of Nb thin films deposited on Pb substrates by pulsed laser deposition as a new concept photocathode for superconductor cavities. Nuclear Instruments and Methods in Physics Research, Section A: Accelerators, Spectrometers, Detectors and Associated Equipment, 2015, 804, 132-136.	0.7	11
51	Novel method for <i>in-situ</i> and simultaneous nanofriction and nanowear characterization of materials. Journal of Vacuum Science and Technology A: Vacuum, Surfaces and Films, 2015, 33, .	0.9	17
52	Piezoelectric and opto-electrical properties of silver-doped ZnO nanorods synthesized by low temperature aqueous chemical method. AIP Advances, 2015, 5, .	0.6	24
53	Tribocorrosion behavior and ions release of CoCrMo alloy coated with a TiAlVCN/CN multilayer in simulated body fluid plus bovine serum albumin. Tribology International, 2015, 81, 159-168.	3.0	41

Advanced Carbon-Based Coatings. , 2014, , 389-412.

#	Article	IF	CITATIONS
55	Reactive sputtering of Î-ZrH2 thin films by high power impulse magnetron sputtering and direct current magnetron sputtering. Journal of Vacuum Science and Technology A: Vacuum, Surfaces and Films, 2014, 32, .	0.9	7
56	ICMCTF 2014 - Preface. Thin Solid Films, 2014, 572, 1.	0.8	0
57	Filtered pulsed cathodic arc deposition of fullerene-like carbon and carbon nitride films. Journal of Applied Physics, 2014, 115, .	1.1	27
58	The effect of oxygen-plasma treatment on the mechanical and piezoelectrical properties of ZnO nanorods. Chemical Physics Letters, 2014, 608, 235-238.	1.2	13
59	Ion beam analysis, corrosion resistance and nanomechanical properties of TiAlCN/CNx multilayer grown by reactive magnetron sputtering. Nuclear Instruments & Methods in Physics Research B, 2014, 331, 134-139.	0.6	8
60	The nature of the frictional force at the macro-, micro-, and nano-scales. Friction, 2014, 2, 40-46.	3.4	41
61	Non-conventional photocathodes based on Cu thin films deposited on Y substrate by sputtering. Nuclear Instruments and Methods in Physics Research, Section A: Accelerators, Spectrometers, Detectors and Associated Equipment, 2014, 752, 27-32.	0.7	2
62	Influence of substrate material on the life of atmospheric plasma sprayed thermal barrier coatings. Surface and Coatings Technology, 2013, 232, 795-803.	2.2	15
63	ICMCTF 2013 — Preface. Thin Solid Films, 2013, 549, 1.	0.8	Ο
64	Comparison of the properties of Pb thin films deposited on Nb substrate using thermal evaporation and pulsed laser deposition techniques. Nuclear Instruments and Methods in Physics Research, Section A: Accelerators, Spectrometers, Detectors and Associated Equipment, 2013, 729, 451-455.	0.7	19
65	Nanoscale piezoelectric response of ZnO nanowires measured using a nanoindentation technique. Physical Chemistry Chemical Physics, 2013, 15, 11113.	1.3	55
66	A Novel Oxide Characterization Method of Nickel Base Alloy 600 Used in Nuclear Plant Reactors. , 2013, , 3355-3361.		2
67	Initial Oxidation of Cu( <i>hkl</i> ) Surfaces Vicinal to Cu(111): A High-Throughput Study of Structure Sensitivity. Journal of Physical Chemistry C, 2012, 116, 16054-16062.	1.5	35
68	Zinc oxide-based thin film functional layers for chemiresistive sensors. Thin Solid Films, 2012, 520, 6669-6676.	0.8	8
69	Differences in the Sliding Wear Track Patterns Between UHMWPE/Steel and UHMWPE/CNx Pairs. , 2012, 1, 329-336.		1
70	Comparative study on the properties of ZnO nanowires and nanocrystalline thin films. Surface and Coatings Technology, 2012, 213, 59-64.	2.2	6
71	Adhesion improvement of carbon-based coatings through a high ionization deposition technique. Journal of Physics: Conference Series, 2012, 370, 012009.	0.3	33
72	Nanoscale elastic modulus of single horizontal ZnO nanorod using nanoindentation experiment. Nanoscale Research Letters, 2012, 7, 146.	3.1	30

Esteban Broitman

#	Article	IF	CITATIONS
73	Highly stable, mesoporous mixed lanthanum–cerium oxides with tailored structure and reducibility. Journal of Materials Science, 2011, 46, 2928-2937.	1.7	35
74	Microstructural evolution of sol–gel derived ZnO thin films. Thin Solid Films, 2010, 518, 6792-6798.	0.8	39
75	Industrial-scale deposition of highly adherent CNx films on steel substrates. Surface and Coatings Technology, 2010, 204, 3349-3357.	2.2	33
76	Oxidation of Fluorinated Amorphous Carbon ( <i>a</i> -CF <sub><i>x</i></sub> ) Films. Langmuir, 2010, 26, 908-914.	1.6	10
77	Water adsorption on phosphorous-carbide thin films. Surface and Coatings Technology, 2009, 204, 1035-1039.	2.2	15
78	Interactions of SO2 and H2S with amorphous carbon films. Applied Catalysis A: General, 2009, 362, 8-13.	2.2	12
79	Dangling bond energetics in carbon nitride and phosphorus carbide thin films with fullerene-like and amorphous structure. Chemical Physics Letters, 2009, 482, 110-113.	1.2	41
80	Characterization of ZnO and ZnO:Al thin films deposited by the sol–gel dip-coating technique. Thin Solid Films, 2008, 517, 1077-1080.	0.8	47
81	Water adsorption on fullerene-like carbon nitride overcoats. Thin Solid Films, 2008, 517, 1106-1110.	0.8	40
82	Fullerene-like Carbon Nitride: A New Carbon-based Tribological Coating. , 2008, , 620-653.		11
83	Oxidation Kinetics of Hydrogenated Amorphous Carbon (a-CHx) Overcoats for Magnetic Data Storage Media. Langmuir, 2007, 23, 5485-5490.	1.6	7
84	Adsorption of Fluorinated Ethers and Alcohols on Fresh and Oxidized Carbon Overcoats for Magnetic Data Storage. Langmuir, 2007, 23, 1953-1958.	1.6	7
85	Electron stimulated decomposition of fluorocarbons on amorphous hydrogenated carbon (a-CHx) overcoats used in data storage media. Tribology Letters, 2007, 26, 45-51.	1.2	2
86	Friction and rolling–sliding wear of DC-pulsed plasma nitrided AISI 410 martensitic stainless steel. Wear, 2006, 260, 479-485.	1.5	53
87	Water adsorption on lubricated fullerene-like CNx films. Thin Solid Films, 2006, 515, 979-983.	0.8	13
88	Carbon nitride as a buffer layer for magnetic thin films. Thin Solid Films, 2005, 476, 148-151.	0.8	0
89	Microstructural and topographical studies of DC-pulsed plasma nitrided AISI 4140 low-alloy steel. Surface and Coatings Technology, 2005, 200, 2391-2397.	2.2	75
90	Microstructure and corrosion behaviour of DC-pulsed plasma nitrided AISI 410 martensitic stainless steel. Surface and Coatings Technology, 2004, 187, 63-69.	2.2	89

Esteban Broitman

#	Article	IF	CITATIONS
91	Structural, mechanical and tribological behavior of fullerene-like and amorphous carbon nitride coatings. Diamond and Related Materials, 2004, 13, 1882-1888.	1.8	76
92	Structural and mechanical properties of diamond-like carbon films deposited by direct current magnetron sputtering. Journal of Vacuum Science and Technology A: Vacuum, Surfaces and Films, 2003, 21, 851-859.	0.9	20
93	Structural, electrical, and optical properties of diamondlike carbon films deposited by dc magnetron sputtering. Journal of Vacuum Science and Technology A: Vacuum, Surfaces and Films, 2003, 21, L23-L27.	0.9	10
94	Mechanical and tribological properties of CNx films deposited by reactive pulsed laser ablation. Diamond and Related Materials, 2002, 11, 98-104.	1.8	29
95	Electrical properties of carbon nitride thin films: Role of morphology and hydrogen content. Journal of Electronic Materials, 2002, 31, L11-L15.	1.0	28
96	Monitoring the structural and chemical properties of CNxthin films during in situ annealing in a TEM. EPJ Applied Physics, 2001, 13, 97-105.	0.3	10
97	Effect of chemical sputtering on the growth and structural evolution of magnetron sputtered CNx thin films. Thin Solid Films, 2001, 382, 146-152.	0.8	94
98	Structural properties of AlSn thin films deposited by magnetron sputtering. Journal of Materials Science Letters, 2001, 20, 1365-1367.	0.5	5
99	Mechanical and tribological properties of CNx films deposited by reactive magnetron sputtering. Wear, 2001, 248, 55-64.	1.5	94
100	Thermal stability of carbon nitride thin films. Journal of Materials Research, 2001, 16, 3188-3201.	1.2	49
101	Anisotropies in magnetron sputtered carbon nitride thin films. Applied Physics Letters, 2001, 78, 2703-2705.	1.5	11
102	Electrical and optical properties of CNx(0⩽x⩽0.25) films deposited by reactive magnetron sputtering. Journal of Applied Physics, 2001, 89, 1184-1190.	1.1	58
103	Growth of CNx/BN:C multilayer films by magnetron sputtering. Thin Solid Films, 2000, 360, 17-23.	0.8	20
104	Growth, structure, and mechanical properties of CN[sub x]H[sub y] films deposited by dc magnetron sputtering in N[sub 2]/Ar/H[sub 2] discharges. Journal of Vacuum Science and Technology A: Vacuum, Surfaces and Films, 2000, 18, 2349.	0.9	48
105	Chemical bonding, structure, and hardness of carbon nitride thin films. Diamond and Related Materials, 2000, 9, 1790-1794.	1.8	14
106	Carbon nitride films on orthopedic substrates. Diamond and Related Materials, 2000, 9, 1984-1991.	1.8	61
107	Influence of plasma parameters on the growth and properties of magnetron sputtered CNx thin films. Journal of Applied Physics, 2000, 88, 524-532.	1.1	74
108	Carbon nitride nanotubulite – densely-packed and well-aligned tubular nanostructures. Chemical Physics Letters, 1999, 300, 695-700.	1.2	137

ESTEBAN BROITMAN

#	Article	IF	CITATIONS
109	Role of nitrogen in the formation of hard and elasticCNxthin films by reactive magnetron sputtering. Physical Review B, 1999, 59, 5162-5169.	1.1	446
110	Ion-plated discontinuous thin film strain gauges. Thin Solid Films, 1998, 317, 440-442.	0.8	13
111	Stress development during deposition of CNx thin films. Applied Physics Letters, 1998, 72, 2532-2534.	1.5	52
112	Reactive magnetron sputtering of CNx thin films at different substrate bias. Thin Solid Films, 1997, 308-309, 223-227.	0.8	41
113	Resistance adjustment in RuO2-based thick film strain-gauges by laser irradiation. Journal of Materials Science Letters, 1997, 16, 1983-1985.	0.5	6
114	Deviations from Matthiessen's rule in continuous metal films. Thin Solid Films, 1996, 277, 192-195.	0.8	8
115	Reactive magnetron sputter deposited CNx: Effects of N2 pressure and growth temperature on film composition, bonding, and microstructure. Journal of Vacuum Science and Technology A: Vacuum, Surfaces and Films, 1996, 14, 2696-2701.	0.9	172
116	Deposition of Y2O3 by plasma enhanced organometallic chemical vapor deposition using an electron cyclotron resonance source. Journal of Vacuum Science and Technology A: Vacuum, Surfaces and Films, 1993, 11, 1870-1874.	0.9	22
117	Order twins in (111)-evaporated thin films of CuAu I. Thin Solid Films, 1990, 191, 275-282.	0.8	0
118	The growth of single-crystal films of silver on rock salt by ion plating. Thin Solid Films, 1988, 165, L101-L105.	0.8	4
119	Structural and Mechanical Properties of CN <sub>X </sub> and CP <sub>X </sub> Thin Solid Films. Key Engineering Materials, 0, 488-489, 581-584.	0.4	2
120	Nano-Scale Friction of Multi-Phase Powder Metallurgy Tool Steels. Advanced Materials Research, 0, 1119, 70-74.	0.3	3